Journal of Hazardous Materials 162 (2009) 682–687

Contents lists available at ScienceDirect

Journal of Hazardous Materials

journal homepage: www.elsevier.com/locate/jhazmat

Decolorization of molasses fermentation wastewater by SnO_2-catalyzed ozonation

Yu-Feng Zeng[a,b], Zi-Li Liu[a,c,*], Zu-Zeng Qin[a]

[a] School of Chemistry & Chemical Engineering, Guangxi University, Nanning 530004, Guangxi, China
[b] Yulin Normal University, Yulin 537000, Guangxi, China
[c] School of Chemistry & Chemical Engineering, Guangzhou University, Guangzhou 510006, Guangdong, China

ARTICLE INFO

Article history:
Received 2 January 2008
Received in revised form 19 May 2008
Accepted 20 May 2008
Available online 24 May 2008

Keywords:
Tin oxide
Catalyzed ozonation
Molasses fermentation wastewater
Decolorization

ABSTRACT

In the presence of O_3, the oxidative decolorization reaction on molasses fermentation wastewater with SnO_2 as a catalyst was studied. The results showed that SnO_2 accelerated the ozone oxidation reaction and the oxidative decolorization of molasses fermentation wastewater was accelerated. Influences on SnO_2 catalytic ozonation activity by precipitants and the calcination temperature were studied by XRD, IR and TG–DSC. SnO_2 prepared by ammonia as the precipitant had higher catalytic activity and a stronger dehydroxylation. The IR spectra of adsorbed pyridine showed that there were Lewis acid sites on the surface of this SnO_2 catalyst. The main factors influencing molasses fermentation wastewater oxidative decolorization were the wastewater concentration, the O_3 concentration, the pH value and the catalyst dosage. The decolorization of wastewater was improved with the increase of the wastewater dilution ratio, the ozone concentration and the catalyst dosage. High activity •OH was found to be existing with less amount and low concentration in the process of SnO_2 catalyzed ozonation decolorization.

1. Introduction

It has been a serious environmental concern that large volume of high strength wastewater has been generated by molasses alcohol manufacturers. Molasses fermentation wastewater is a kind of high concentration organic acidity wastewater, discharged after alcohol is extracted in distillation tower by fermented molasses. The wastewater is characterized by very high chemical oxygen demand (COD) (65 000–130 000 mg L^{-1}) and biochemical oxygen demand (BOD_5) (30 000–96 000 mg L^{-1}) and has a bad smell and dark brown color. The main components of molasses fermentation wastewater are the melanin browning caused by polyphenols, the polymer melanin caused by reaction of decomposed condensation polymerization with reduced sugar alkali, Maillard pigment, caramel, and large amount of carbonate and phosphate. Since this kind of pigments is heat and light resistant, and has not been decolorized for a long time, it is difficult to destroy them by biochemical and physico-chemical methods [1,2].

Because of its strong oxidation capacity, ozone has been applied to degrade molasses fermentation wastewater [3–5], but the utilization ratio of ozone was not high. It is an effective method to strengthen the ozone oxidation process with catalyst [6]. There are homogeneous catalytic ozone oxidation and heterogeneous catalytic ozone oxidation. Heterogeneous catalysis is the most promising process of wastewater treatment because its low cost, its catalyst reclamation capability, and its lack of secondary pollution. At present, heterogeneous catalytic ozonation process has been reported in several papers and metal-oxide (MnO_2 [7–10], Al_2O_3 [11,12], TiO_2 [13–15]) and supported metal or metal oxides [16–18] and activated carbon [19–21] have been used as ozonation catalysts.

Tin (IV) oxide (SnO_2) is an n-type semiconductor material with wide band gap energy, high donor concentration and large mobility [22]. However, no study on SnO_2 catalytic ozonation has been reported.

This paper focuses on the use of SnO_2 catalyst to treat the molasses fermentation wastewater in the presence of O_3. The process of oxidative decolorization was studied and a preliminary review on the mechanism of catalytic ozonation reaction was presented as well.

2. Experimental

2.1. Materials

$SnCl_4{\cdot}5H_2O$ and NH_4OH were prepared in certain concentrations. NH_4OH solution was added drop-wise to the $SnCl_4$ solution,

* Corresponding author at: School of Chemistry & Chemical Engineering, Guangxi University, Nanning 530004, Guangxi, China. Tel.: +86 20 39366904.
E-mail address: gzdxlzl@gmail.com (Z.-L. Liu).

0304-3894/$ – see front matter © 2008 Elsevier B.V. All rights reserved.
doi:10.1016/j.jhazmat.2008.05.094

and the mixture was adjusted to pH 8 and stirred to yield a white precipitate. After being grounded under 353 K for 3 h, the precipitate was filtered and washed with distilled water until no chloride ion was detected in the filtrate (0.5 mol L^{-1} $AgNO_3$ solution was used as the detector). Then the material was dried for 10 h at 383 K, resulting in a SnO_2 precursor. The precursor was grounded to pass through a 100-mesh sieve mesh and calcined for 2 h at different temperatures in a muffle furnace to obtain the SnO_2 catalyst.

Molasses fermentation wastewater was obtained from Nannin Pumiao Sugar Plant. The wastewater is dark brown in color, with absorbance unit of 2.14 at 475 nm after 10 times dilution. Other characteristics of molasses fermentation wastewater were COD 9.5×10^4 mg L^{-1}, BOD_5 2.2×10^4 mg L^{-1}, SS 3.53×10^4 mg L^{-1} and pH 4.12.

2.2. Experimental setup

The catalytic ozonation process of molasses fermentation wastewater decolorization was a standard ozonation experimental setup. The reaction was preceded at room temperature and 200 mL 10% (v/v) wastewater and certain amount of catalyst were added into the ozone reactor. The reactor was sealed up in the entire reaction process. When the experiment started, the air pump and magnetic stirrer were turned on and the rotameter was regulated to control air flow in a steady rate. Then the ozone generator was turned on. The ozone flowed into the ozone reactor and then the catalytic ozonation reaction started. The reaction off-gas flowed into 2% KI absorption solution through the buffer bottle and then was evacuated. The pH value for the liquid in this process was the initial pH value of molasses fermentation wastewater if not designated.

2.3. Analytical methods and SnO_2 characterization

After the catalytic ozonation reaction, 10 mL solution was centrifuged for 10 min at 3000 rpm, and then the solution absorbance was measured. The change in the wastewater absorbance at 475 nm [3–5] was detected with a TU1901 UV–vis spectrophotometer (Beijing Purkinje General Instrument Co. Ltd.). The decolorization rate equation was decolorization (%) = $(A_0 - A)/A_0 \times 100$, where A_0: the absorbance of the initial solution; A: the absorbance of the solution in different reaction stage.

XRD measurements were carried out by a MASAL XD-3 X-ray diffractometer with Cu Kα radiation (36 kV, 20 mA) (Beijing Purkinje General Instrument Co. Ltd.) and this system was operated with a continuous scan mode (4° min^{-1}) to get diffraction data between 15° and 90°.

TG–DSC of the SnO_2 catalyst was measured on a SDT Q600 thermal analyzer (TA Instruments). The experiment was preceded with a carrier gas of 100 mL min^{-1} nitrogen, and tested between 323 and 1273 K with a rate of 20 K min^{-1}.

The surface acidity of SnO_2 catalyst was studied by pyridine adsorption infrared spectrometer in a Nicolet NEXUS 470 infrared spectrometer. The catalyst was swept by argon at 693 K for 1 h, then cooled to room temperature and then heated to 473 K and finally flowed into the steam pyridine. The steam pyridine was absorbed at 473 K, and then the data was recorded.

The infrared spectrum of ozone absorbed on SnO_2 surface was studied in a Nicolet NEXUS 470 infrared spectrometer. SnO_2 was pressed to tablet after being dispersed in a KBr matrix. The spectrometer scanned 20 times at a resolution of 4 cm^{-1}, and scanned from 400 to 4000 cm^{-1} with the mirror phase velocity of 0.6329. Ozone generated from the air in the ozone generator flowed into the sample pool and was absorbed for 15 min at room temperature and pressure, and then the infrared spectrum data were recorded.

3. Results and discussion

3.1. Catalytic activities

3.1.1. Effect of precipitants

The catalytic ozonation was proceeded in 200 mL molasses fermentation wastewater at an air flow rate of 80 L h^{-1} to generate ozone. 2.5 g L^{-1} SnO_2 was added, which was prepared by NH_4OH, Na_2CO_3 and NaOH, respectively. The influence of precipitants on molasses fermentation wastewater decolorization by SnO_2 catalytic ozonation was shown in Fig. 1.

After a 60-min catalytic ozonation reaction, the yields of wastewater decolorization by SnO_2 prepared by NH_4OH, Na_2CO_3 and NaOH were 60.24%, 44.22% and 49.72%, respectively. By contrast, the decolorization yield by ozone oxidation without SnO_2 catalyst is only 43.04%. After a reaction for 15, 30 and 45 min, the wastewater decolorization yield by SnO_2 prepared by NH_4OH was 15% more than that by the other two methods. These results show that SnO_2 as a catalyst has different catalytic effects with different precipitants and SnO_2 prepared by NH_4OH had the highest catalytic activity.

3.1.2. Structures of SnO_2 catalysts prepared by different precipitants

The XRD patterns of SnO_2 catalyst prepared by different precipitants were shown in Fig. 2.

In Fig. 2, the three patterns were basically the same, and the intensity and position of the diffraction peaks at $2\theta = 26.7°$ (1 1 0), 33.9° (1 0 1), and 52.0° (2 1 0) were the same as the JCPDS standard (41-1445), which indicates that SnO_2 crystal can be prepared by any of these three different precipitants. And the particle sizes of SnO_2 (1 1 0-lattice plane), which were calculated by Scherrer equation: $D = k\lambda/\beta \cos\theta$, were 7, 24 and 11 nm, respectively. The particle sizes of SnO_2 prepared by NH_4OH showed in SEM image (not shown here) was about 2 μm. However, there were two diffraction peaks at $2\theta = 31.9°$ and 45.6° of the catalysts prepared by Na_2CO_3 and NaOH as precipitant. Compared to the JCPDS standard pattern, these two peaks were the 2 0 0 and 2 2 0-lattice plane of NaCl respectively, which indicates that there was NaCl in the SnO_2 prepared by Na_2CO_3 and NaOH and that the catalytic activity of SnO_2 may be decreased consequently and might cause the decrease of the decolorization yield of molasses fermentation wastewater.

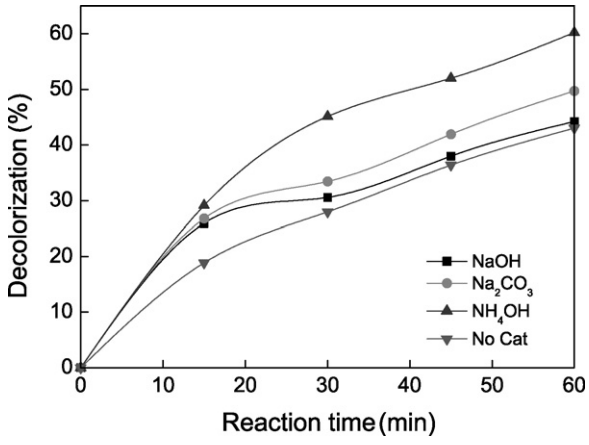

Fig. 1. Influence of precipitants on molasses fermentation wastewater decolorization by SnO_2 catalytic ozonation.

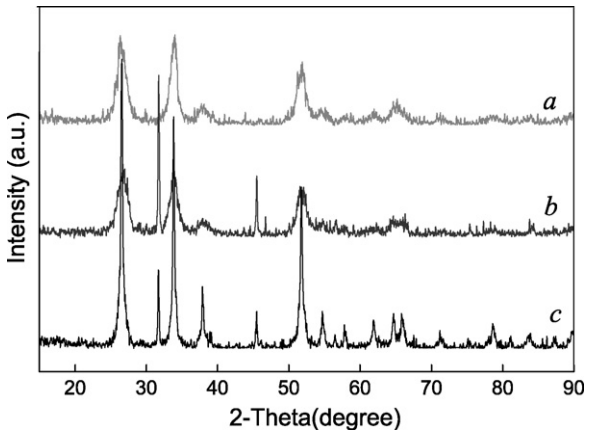

Fig. 2. XRD patterns of SnO_2 prepared by (a) NH_4OH, (b) Na_2CO_3 and (c) NaOH as precipitant.

3.2. TG–DSC analysis of different catalyst precursors

SnO_2 precursors prepared by different precipitants were preceded with TG–DSC analysis by a thermal analyzer, and the results were shown in Fig. 3.

In Fig. 3(a), SnO_2 precursor prepared by NH_4OH exhibited two significant thermo weight-loss processes between 430 and 580 K. One process was between 430 and 536 K with a weight loss of 41.8%, which was attributed to the weight loss of crystal water and the decomposition of residuary NH_4Cl that was not washed out in the prepared process. The maximum weight-loss rate temperature of SnO_2 was 529 K in this process.

The other process was between 536 and 580 K with a weight loss of 28.3%, and the maximum weight-loss rate temperature was 553 K. This process should be the process in which the precursor hydroxyl group was removed and SnO_2 was formed [23].

$$Sn(OH)_4 \rightarrow SnO_2 + 2H_2O \quad (1)$$

If the precursor was $Sn(OH)_4$, and Eq. (1) was used for the calculation, then the weight loss in this experiment was 19.3%, which was more than the theoretical value of 9%. Previous studies showed that the decomposition temperature of $Sn(OH)_4$ was around 618.8 K [24] and that the decomposition temperature would decrease if there were some other impurities whose structure changed the thermodynamic and kinetic rules. Therefore, in addition to the decomposition of $Sn(OH)_4$, there must be crystal water loss and NH_4Cl decomposition in this process. As Fig. 3(a) indicates, SnO_2 precursor prepared by NH_4OH was decomposed completely below 580 K and in the weight loss process, there were two endothermic peaks at 532 and 556 K, which shows that the precursor absorbed heat at the above temperature and was then decomposed. Moreover, the exothermic peak above 600 K indicated that the powder changed from amorphous state to crystalline state in the process of heating.

In Fig. 3(b) and (c), the weight loss of SnO_2 precursor prepared by $NaCO_3$ and NaOH were lower than that prepared NH_4OH. When $NaCO_3$ and NaOH were used as the precipitants, the maximum weight-loss rate for physical absorbed water removal was achieved when the temperature was 350 and 361 K, respectively and the temperature range for hydroxyl group removal was 423 to 693 K. Since there was a large amount of NaCl in these two precursors, as the previous XRD analysis indicates, the weight loss rate of these two precursors was slower. The peaks of the DSC curves were flatter, which indicated that the extent of hydroxyl group removal was weaker and that less activity centers were formed. Accordingly, there were significant differences in terms of the catalytic activity of SnO_2 prepared by these three precipitants calcined at 723 K

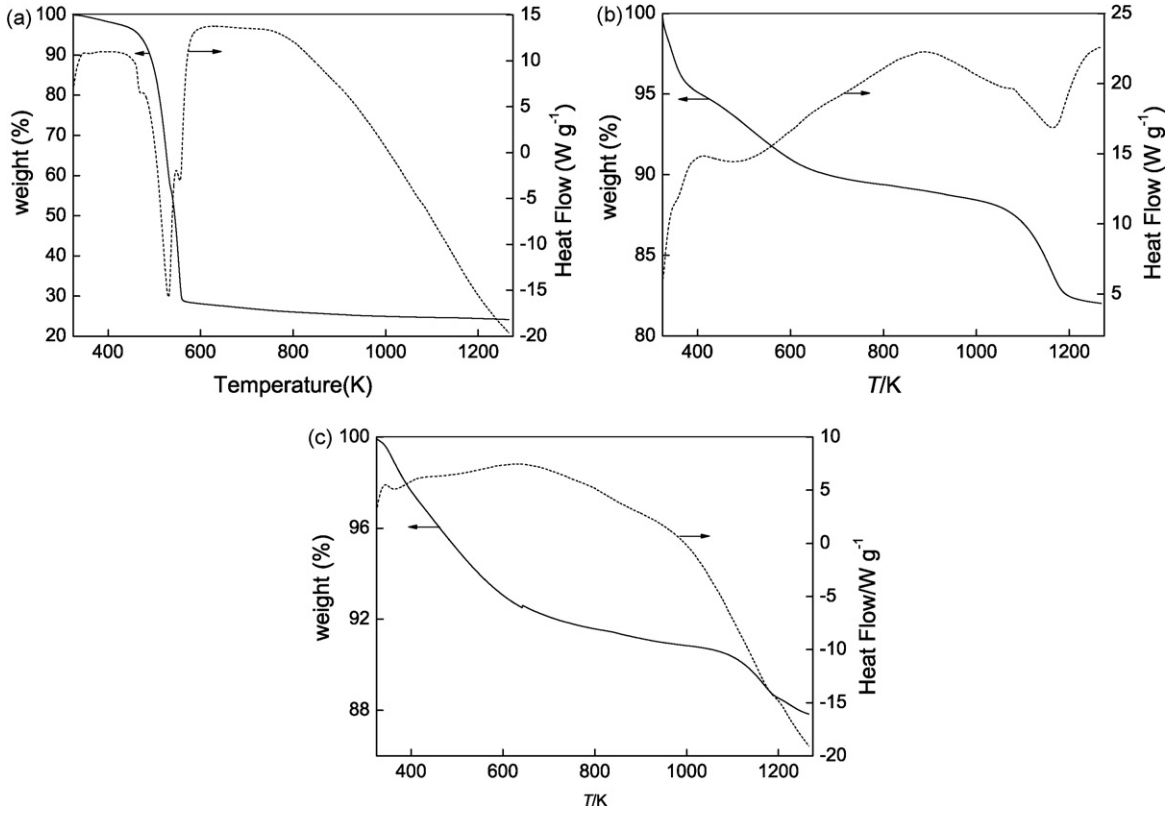

Fig. 3. TG–DSC of SnO_2 precursor prepared by (a) NH_4OH, (b) Na_2CO_3 and (c) NaOH as precipitant.

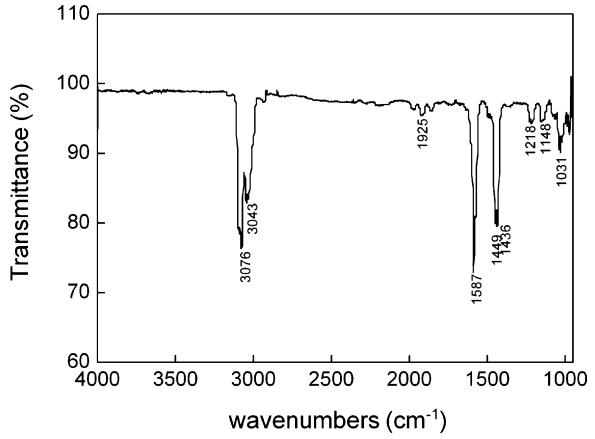

Fig. 4. IR spectrum of pyridine absorbed on SnO_2.

for 2 h, and SnO_2 prepared by NH_4OH had higher catalytic activity.

3.3. Surface acidity of SnO_2

SnO_2 is a kind of multifunction catalyst with different activity sites. The acidity site is one of the most important activity centers, so it is necessary to investigate the surface acidity of SnO_2. Pyridine is the most commonly used basic probe molecule for surface acidity characterization [25]. The surface acidity of SnO_2 was investigated by pyridine absorbed on SnO_2 surface with FT-IR spectroscopy. The results were shown in Fig. 4.

According to other researches [26], interference of physical adsorption will be excluded above 473 K while pyridine is used as a probe molecular to research surface acidity, and the exact information of proton acid and Lewis acid can be obtained. Therefore, our experiment was proceeded with the pyridine gas at 473 K. The spectrum shows several bands in Fig. 5: two peaks at 3076 and 3043 cm^{-1} assigned to ν_{C-H}, which was the stretching vibration of pyridine molecular hexatomic ring and two peaks at 1587 cm^{-1} (ν_{C-C}) and 1577 cm^{-1} (ν_{C-N}) assigned to the vibration adsorption band of pyridine hydrogen bond. The absorption peak at 1449 cm^{-1} (ν_{19b}) was formed of vibration of molecular flat hexatomic ring, which took place between pyridine molecular and Lewis acid sites of Sn^{4+}on catalyst surface [25]; 1436 cm^{-1} may be the physical absorption peak of pyridine. When pyridine was absorbed, characteristic peaks of Brønsted acid site are located at ~1540 and 1640 cm^{-1}, and characteristic peaks Lewis acid site are located at ~1450 and 1620 cm^{-1} [27]. According to the spectrum in Fig. 4, only Lewis acid site was present on the catalyst surface.

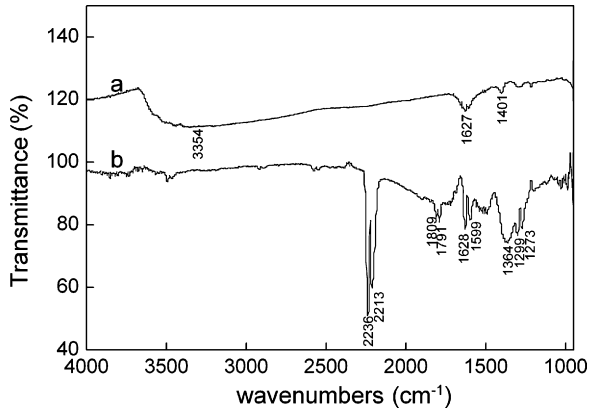

Fig. 5. IR spectrum of (a) SnO_2 and (b) ozone adsorbed on SnO_2 for 15 min.

3.4. Ozone adsorption on the surface of SnO_2

The IR spectrum (Fig. 5) of O_3 absorbed on SnO_2 surface was conducted at room pressure and room temperature, which was compatible with the SnO_2 catalyzed ozonation of wastewater. Ozone was prepared from air.

The infrared transmission spectrum of SnO_2 without treatment is shown in Fig. 5(a) and it indicates that there are three absorption peaks: 3354 cm^{-1} assigned to the stretching vibration of Sn—OH, 1627 cm^{-1} assigned to the bending vibration of hydroxyl, and 1041 cm^{-1} assigned the stretching vibration of Sn—O—Sn [28]. Fig. 5(b) shows the IR spectrum of ozone absorbed on SnO_2 surface. The IR spectrum of pyridine absorbed on SnO_2, discussed above, indicated that there was the activity centre of Lewis acid sites on the catalyst surface (in Section 3.3). On the IR spectrum of ozone adsorbed on SnO_2, the peaks of 2236 and 2213 cm^{-1} were the absorption peaks of CO and O_3 adsorbed on SnO_2 at Lewis acid activity sites. The peaks at 1809 and 1791 cm^{-1} were the stretching vibration peaks of C=O bond. The peak at 1628 cm^{-1} is due to the bending vibration of H—O—H and that at 1599 cm^{-1} is due to the stretching vibration of C=C bond. The peak at 1364 cm^{-1} was the characteristic absorption peak of O_2 or CO, and the double peak of 1299 and 1273 cm^{-1} was the ozone characteristic absorption peak. The surface adsorption becomes more complex and the reason may be that NO_x and CO are present in the ozone prepared from air [28–30]. There are two main methods of ozone adsorption on the surface of metal oxide [28–34]: one is the bond formation reaction between surface hydroxyl of metal oxide and terminal oxygen atom of ozone and the other is the bond formation reaction between Lewis acid activity site of metal oxide and terminal oxygen atom of ozone.

3.5. Study on the process of SnO_2 catalyzed ozonation

3.5.1. Effect of initial pH

The effect of pH on the SnO_2 catalytic ozonation decolorization was investigated at room temperature with the pH range of 3–13 and the 2.50 g L^{-1} SnO_2 catalyst. The effect of the initial pH on the SnO_2-catalyzed ozonation decolorization and COD removal were shown in Fig. 6.

Under acidic conditions, direct reaction between the ozone molecular and a particular group takes place selectively while

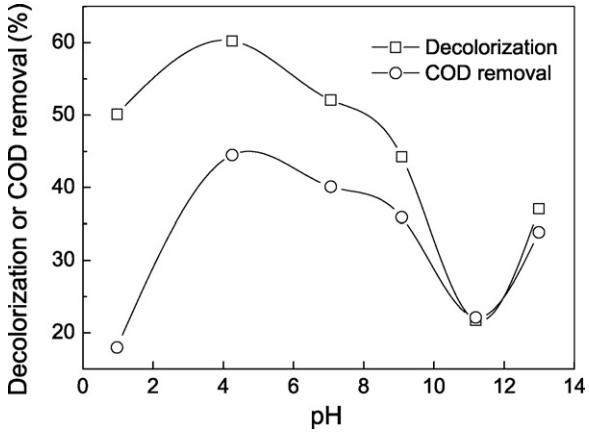

Fig. 6. Influence of pH on decolorization and COD removal of molasses fermentation wastewater.

under alkaline conditions OH^- is broken down into high activity •OH whose oxidation potential is higher than the non-selectivity •OH of ozone [23]. As Fig. 6 shows, when the pH value was 4.25 (the pH value of molasses fermentation wastewater after being diluted 10 times), the decolorization yield of wastewater reached the highest rate of 60.24%. At the same condition, the COD was decreased from 914 to 507 mg L^{-1}(the molasses fermentation wastewater was diluted 10 times). The COD removal was 44.5%, which was the highest COD removal at different pH. The addition of SnO_2 accelerated the direct reaction between ozone and organic substance in wastewater. When the pH value was 11, the lowest decolorization yield was 21%, which was the lowest. The COD removal was only 22.3%. At this pH value, the existing CO_3^{2-}, HPO_4^{2-}, which were free radical scavengers, were more dominant than HCO^{3-}, H_2PO_4 [24], which caused the reduction of radicals and thus the decrease in the decolorization yield and COD removal. However, when the pH value was above 11, the decolorization yield of wastewater was slightly increased. To sum up, under acidic conditions, the effect of pH on catalyzed ozonation degradation of molasses fermentation wastewater was significant.

3.5.2. Effect of the air flow rate

The amount of ozone, which was generated by the ozone generator, was increased with the increase of air flow. The ozone flow was improved from 27.38 to 230.28 mg L^{-1} h^{-1} with the air flow increased from 40 to 120 L h^{-1}. Different ozone concentrations had different effects on the decolorization yield of wastewater. The influence of the airflow on the decolorization of molasses fermentation wastewater was shown in Fig. 7.

When the air flow rate was increased from 40 to 120 L h^{-1}, after 60 min, the decolorization yield of molasses fermentation wastewater was increased from 42.66% to 71.85% by SnO_2 catalyzed ozonation. When the air flow rate was below 100 L h^{-1}, the yield of decolorization by SnO_2 catalyzed ozonation was about 10% higher than that by ozone oxidation alone. The amount of ozone was significantly increased at the airflow rate of 120 L h^{-1}. However, the organic compounds in the wastewater reacted with large amount of ozone directly and the catalytic function of SnO_2 did not have a full display on the degradation of molasses fermentation wastewater. Taking into account the energy consumption, the catalytic efficiency and the damage of the ozone generator, the optimal air flow rate was 80 L h^{-1}.

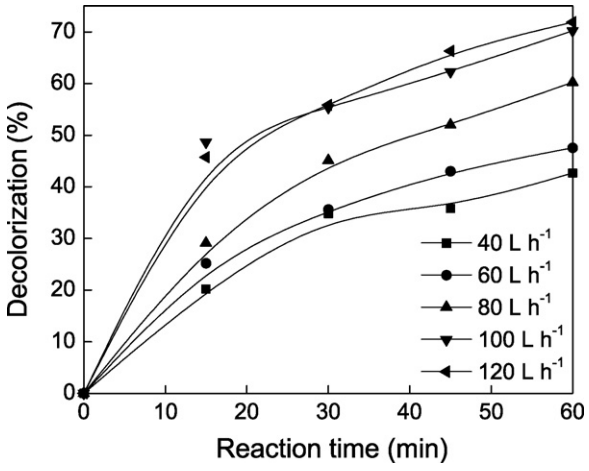

Fig. 7. Influence of air flow on decolorization of molasses fermentation wastewater.

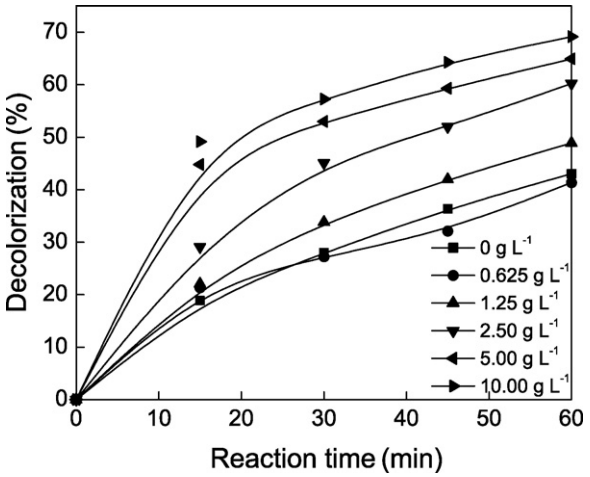

Fig. 8. Influence of catalyst dose on decolorization of molasses fermentation wastewater.

3.5.3. Effect of catalyst dosage

The influence of the catalyst dosage on the decolorization of molasses fermentation wastewater was given in Fig. 8, where the airflow rate was 80 L h^{-1} and the wastewater dilution ratio was 1:10.

According to Fig. 8, when 0.625 g L^{-1} SnO_2 was added, the decolorization yield of wastewater had no significant change compared with that without the catalyst, which showed that ozone oxidation could not be enhanced at this amount of catalyst. After the addition amount of SnO_2 was above 1.25 g L^{-1}, the decolorization yield of molasses fermentation wastewater was obviously higher than that with the previous amount, which may be related to O_3 absorbed on the surface of SnO_2 catalyst. The adsorption quantity of organic compounds and O_3 was increased with the increase of the addition amount of the catalyst, and the reaction on the catalyst surface was also increased, which caused the increase of the degradation. Although the degradation was increased with the increase of the addition amount of SnO_2, a big addition of catalyst would cause a series of problems such as the difficulty to separate and recover the catalyst, and the increase of wastewater treatment cost. Therefore, the optimal SnO_2 additive amount was 2.50 g L^{-1}.

3.6. The primary mechanism of the SnO_2-catalyzed ozonation

Ozone oxidation is always a kind of free radical reaction and thus free radical scavengers existing in the wastewater have obvious effects on the decolorization of wastewater by ozone oxidation [6]. *Tert*-Butyl alcohol is stable under the neutral and acidic conditions, and the reaction constant ($k = 5 \times 108$ L mol^{-1} s^{-1}) between *tert*-butyl alcohol and ·OH is very large. Therefore, *tert*-butyl alcohol is always used as the free radical scavenger. In our experiment, the dilution ratio of wastewater was 1:20, and 2.5 g L^{-1} SnO_2 catalyst and 10 mg L^{-1} *tert*-butyl alcohol was added. The influence of *tert*-butyl alcohol on the decolorization of wastewater by SnO_2 catalyzed ozonation was investigated, and the result was shown in Fig. 9.

According to Fig. 9, the decolorization yield of molasses fermentation wastewater was decreased with the presence of tert-butyl alcohol, which indicated that the oxidation decolorization reaction was inhibited by the free radical scavenger of tert-butyl alcohol. It also showed that there was ·OH in this reaction system. However, the decolorization yield of wastewater was only decreased 8%, which implies that the quantity of •OH, which was scavenged by *tert*-butyl alcohol, is little, and the high concentra-

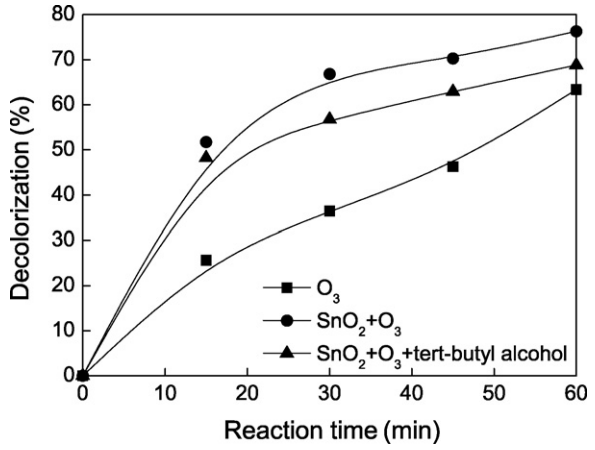

Fig. 9. Influence of *tert*-butyl alcohol on SnO_2-catalyzed ozonation.

tion O_3 and the organic compounds in the wastewater reacted directly.

4. Conclusions

(1) The ozonation catalytic activity of SnO_2 prepared by NH_4OH was higher than SnO_2 prepared by NaOH or Na_2CO_3.
(2) The decolorization yield of molasses fermentation wastewater was improved by increasing the dilution ratio of molasses fermentation wastewater, the O_3 concentration and the catalyst dosage. The reaction time had no obvious effect on the decolorization of wastewater, but the pH value of reactant had significant effect on the decolorization of wastewater. The appropriate conditions were a dilution ratio of 1:10 for molasses fermentation wastewater, an airflow rate of 80 L h^{-1}, a catalyst dosage of 2.5 g L^{-1} and a pH of 4.2 for the wastewater, and the decolorization rate was 60.2% under the reaction condition within 60 min.
(3) High activity ·OH was found to have a less amount and low concentration in the process of SnO_2 catalyzed ozonation decolorization. In addition, the direct ozone oxidative reaction of ozone and the organism in the wastewater was dominant in the oxidation reaction.

Acknowledgments

The project was supported by National Natural Science Foundation of China (No. 20466001), Guangxi University Key Program for Science and Technology Research (No. 2004ZD01) and Guangzhou Education office Scientific Research Project (No. 62040).

References

[1] C. Guimarães, L.S.M. Bento, M. Mota, Biodegradation of colorants in refinery effluents: potential use of the fungus *Phanerochaete chrysosporium*, Int. Sugar J. 101 (1999) 246–251.
[2] G.G. Benito, M.P. Miranda, M.T.G. Cubero, M.A.U. Alonso, Decolorization of molasses effluents by coagulation–flocculation process, Sugar Ind. 124 (1999) 406–410.
[3] M. Coca, M. Pena, G. Gonzalez, Variables affecting efficiency of molasses fermentation wastewater ozonation, Chemosphere 60 (2005) 1408–1415.
[4] M. Coca, M. Pena, G. Gonzalez, Kinetic study of ozonation of molasses fermentation wastewater, J. Hazard. Mater. 149 (2007) 364–370.
[5] M. Pena, M. Coca, G. Gonzalez, R. Rioja, M.T. Garcia, Chemical oxidation of wastewater from molasses fermentation with ozone, Chemosphere 51 (2003) 893–900.
[6] B. Kasprzyk-Hordern, M. Ziolek, J. Nawrocki, Catalytic ozonation and methods of enhancing molecular ozone reactions in water treatment, Appl. Catal. B 46 (2003) 639–669.
[7] R. Andreozzi, V. Caprio, R. Marotta, V. Tufano, Kinetic modeling of pyruvic acid ozonation in aqueous solutions catalyzed by Mn(II) and Mn(IV) ions, Water Res. 35 (2001) 109–120.
[8] S.-P. Tong, W.-P. Liu, W.-H. Leng, Q.-Q. Zhang, Characteristics of MnO_2 catalytic ozonation of sulfosalicylic acid and propionic acid in water, Chemosphere 50 (2003) 1359–1364.
[9] J. Ma, N.J.D. Graham, Degradation of atrazine by manganese-catalysed ozonation—influence of radical scavengers, Water Res. 34 (2000) 3822–3828.
[10] R. Andreozzi, M.S. Lo Casale, R. Marotta, G. Pinto, A. Pollio, *N*-Methyl-*p*-aminophenol (metol) ozonation in aqueous solution: kinetics, mechanism and toxicological characterization of ozonized samples, Water Res. 34 (2000) 4419–4429.
[11] C.H. Ni, J.N. Chen, Heterogeneous catalytic ozonation of 2-chlorophenol aqueous solution with alumina as a catalyst, Water Sci. Technol. 43 (2001) 213–220.
[12] M. Ernst, F. Lurot, J.-C. Schrotter, Catalytic ozonation of refractory organic model compounds in aqueous solution by aluminum oxide, Appl. Catal. B 47 (2004) 15–25.
[13] F.J. Beltran, F.J. Rivas, R. Montero-de-Espinosa, Catalytic ozonation of oxalic acid in an aqueous TiO_2 slurry reactor, Appl. Catal. B 39 (2002) 221–231.
[14] F.J. Beltrán, J. Rivas, P. Álvarez, R. Montero-de-Espinosa, Kinetics of heterogeneous catalytic ozone decomposition in water on an activated carbon, Ozone Sci. Eng. 24 (2002) 227–237.
[15] Y. Yang, J. Ma, Q. Qin, X. Zhai, Degradation of nitrobenzene by nano-TiO_2 catalyzed ozonation, J. Mol. Catal. A: Chem. 267 (2007) 41–48.
[16] F. Delanoe, B. Acedo, N. Karpel Vel Leitner, B. Legube, Relationship between the structure of Ru/CeO_2 catalysts and their activity in the catalytic ozonation of succinic acid aqueous solutions, Appl. Catal. B 29 (2001) 315–325.
[17] S.-P. Tong, W.-H. Leng, J.-Q. Zhang, C.-N. Cao, Catalytic ozonation of sulfosalicylic acid, Ozone Sci. Eng. 24 (2002) 117–122.
[18] X. Li, J.-H. Yao, J.-Y. Qi, Degradation of organic pollutants in water by catalytic ozonation, Chem. Res. Chin. Univ. 23 (2007) 273–275.
[19] S.H. Lin, C.L. Lai, Kinetic characteristics of textile wastewater ozonation in fluidized and fixed activated carbon beds, Water Res. 34 (2000) 763–772.
[20] J. Rivera-Utrilla, M. Sanchez-Polo, Ozonation of 1,3,6-naphthalenetrisulphonic acid catalysed by activated carbon in aqueous phase, Appl. Catal. B 39 (2002) 319–329.
[21] X. Qu, J. Zheng, Y. Zhang, Catalytic ozonation of phenolic wastewater with activated carbon fiber in a fluid bed reactor, J. Colloid Interf. Sci. 309 (2007) 429–434.
[22] Z.M. Jarzebski, J.P. Marton, Physical properties of SnO_2 materials, J. Electrochem. Soc. 123 (1976) 199C–205C.
[23] W.H. Glaze, J.W. Kang, Advanced oxidation processes: description of a kinetic model for the oxidation of hazardous materials in aqueous media with ozone and hydrogen peroxide in a semibatch reactor, Ind. Eng. Chem. Res. 28 (1989) 1573–1580.
[24] B. Langlais, D.A. Reckhow, D.R. Brink, Ozone in water treatment: application and engineering, Marcel Dekker, New York, 1991, pp. 85–92.
[25] G. Busca, Spectroscopic characterization of the acid properties of metal oxide catalysts, Catal. Today 41 (1998) 191–206.
[26] M. Cardona, N.J.A. Dumesic, Applications of adsorption microcalorimetry to the study of heterogeneous catalysis, Adv. Catal. (1992) 149–244.
[27] A. Corma, Inorganic solid acids and their use in acid-catalyzed hydrocarbon reactions, Chem. Rev. 95 (1995) 559–614.
[28] D. Amalric-Popescu, F. Bozon-Verduraz, Infrared studies on SnO_2 and Pd/SnO_2, Catal. Today 70 (2001) 139–154.
[29] D. Mehandjiev, A. Naydenov, G. Ivanov, Ozone decomposition, benzene and CO oxidation over $NiMnO_3$–ilmenite and $NiMn_2O_4$–spinel catalysts, Appl. Catal. A 206 (2001) 13–18.
[30] J.P. Viricelle, A. Pauly, L. Mazet, J. Brunet, M. Bouvet, C. Varenne, C. Pijolat, Selectivity improvement of semi-conducting gas sensors by selective filter for atmospheric pollutants detection, Mater. Sci. Eng. C 26 (2006) 186–195.
[31] K.M. Bulanin, J.C. Lavalley, A.A. Tsyganenko, Infrared study of ozone adsorption on TiO_2 (anatase), J. Phys. Chem. 99 (1995) 10294–10298.
[32] K.M. Bulanin, J.C. Lavalley, A.A. Tsyganenko, IR spectra of adsorbed ozone, Colloids Surf. Physicochem. Eng. Aspects 101 (1995) 153–158.
[33] K.M. Bulanin, J.C. Lavalley, A.A. Tsyganenko, Infrared study of ozone adsorption on CaO, J. Phys. Chem. B 101 (1997) 2917–2922.
[34] K.M. Bulanin, J.C. Lavalley, J. Lamotte, L. Mariey, N.M. Tsyganenko, A.A. Tsyganenko, Infrared study of ozone adsorption on CeO_2, J. Phys. Chem. B 102 (1998) 6809–6816.